ELSEVIER

Fusion Engineering and Design 28 (1995) 457–478

Fusion Engineering and Design

Quantification of design margins and safety factors based on the prediction uncertainty in tritium production rate from fusion integral experiments of the USDOE/JAERI collaborative program on fusion blanket neutronics

M.Z. Youssef [a], A. Kumar [a], M.A. Abdou [a], Y. Oyama [b], C. Konno [b], F. Maekawa [b], Y. Ikeda [b], K. Kosako [b], M. Nakagawa [b], T. Mori [b], H. Maekawa [b]

[a] *Mechanical, Aerospace, and Nuclear Engineering Department, School of Engineering and Applied Science, University of California at Los Angeles, Los Angeles, CA 90024, USA*

[b] *Department of Reactor Engineering, Tokai Research Establishment, Japan Atomic Energy Research Institute, Tokai-mura, Naka-gun, Ibaraki-ken, Japan*

Abstract

Several fusion integral experiments were performed within a collaboration between the USA and Japan on fusion breeder neutronics aimed at verifying the prediction accuracy of key neutronics parameters in a fusion reactor blanket based on current neutron transport codes and basic nuclear databases. The focus has been on the tritium production rate (TRP) as an important design parameter to resolve the issue of tritium self-sufficiency in a fusion reactor. In this paper, the calculational and experimental uncertainties (errors) in local TPR in each experiment performed i were interpolated and propagated to estimate the prediction uncertainty u_i in the line-integrated TPR and its standard deviation σ_i. The measured data are based on Li-glass and NE213 detectors. From the quantities u_i and σ_i, normalized density functions (NDFs) were constructed, considering all the experiments and their associated analyses performed independently by the UCLA and JAERI. Several statistical parameters were derived, including the mean prediction uncertainties $\bar{u}$ and the possible spread $\pm\sigma_u$ around them. Design margins and safety factors were derived from these NDFs. Distinction was made between the results obtained by UCLA and JAERI and between calculational results based on the discrete ordinates and Monte Carlo methods. The prediction uncertainties, their standard deviations and the design margins and safety factors were derived for the line-integrated TPR from Li-6 T_6, and Li-7 T_7. These parameters were used to estimate the corresponding uncertainties and safety factor for the line-integrated TPR from natural lithium T_n.

1. Introduction

Validation of the nuclear performance of the first-wall(FW)/blanket/shield system in a fusion reactor prior to construction is a necessary step to meet the regulatory and licensing (or construction authorization) requirements and to ensure meeting certain design requirements for particular responses. The responses of prominent interest are the tritium production rate (TPR), the bulk shield attenuation characteristics, dose

SSDI 0920-3796(94)00162-6

around streaming paths, induced activation and decay heat. Thus, the needed research and development effort should have the objectives of (1) providing the experimental databases required for approval and licensing of the device prior to construction, (2) verifying the prediction capabilities of present calculational tools and databases for the purpose of code verification and data certification, (3) generation of design safety factors to assist designers in implementing conservatism in component design for higher reliability, and (4) reducing the high cost associated with untested large safety factors commonly used to compensate for all sources of uncertainties.

The purpose of this paper is to quantify the current prediction uncertainty in the line-integrated TPR in a typical fusion blanket by comparing predicted values with measured data obtained from dedicated integral experiments that closely simulate the fusion environment in terms of material selection and source conditions. Quantifying the uncertainties in the TPR is central to examining the critical issue of tritium self-sufficiency in fusion reactors based on the D–T fuel cycle [1,2]. The results from the USDOE/JAERI Collaborative Program on Fusion Blanket Neutronics were extensively used for that purpose, focusing on items (1)–(4) above, to arrive at estimates for the design margins and safety factors based on the observed discrepancies between calculations and measurements. The present work is based on measurements performed using Li-glass and NE213 detectors to measure the TPR from Li-6 T_6 and Li-7 T_7 respectively. Parallel work based on other measuring techniques have been previously reported and can be found in Refs. [3,4]. The approach used to generate the design margins and correction factors is described in Section 2. A brief description of the integral experiments is given in Section 3. The calculational tools and databases used independently by the US and Japan to analyze these experiments are described in Section 4. Estimates of the derived design margins and correction factors, along with the associated confidence levels, are given in Section 5. General conclusions are discussed in Section 6.

2. Theoretical approach

The methodology followed to derive design margins and safety factors from the calculational and experimental results for several experiments was previously developed and described in Ref. [3]. We briefly outline here this theoretical approach for completeness. Suppose we have the calculational and experimental results from a number N of experiments. In a given experiment i, a particular integral response R has a calculated value c_i, and a measured value e_i. Ideally, the ratio c_i/e_i will be equal to unity if the calculational method and modeling used to arrive at c_i are exact using the most accurate database and if no experimental errors are encountered. In practice, this ratio deviates from unity by a fraction, $u_i = c_i/e_i - 1$, defined as the prediction uncertainty in the response R, owing to the approximations embedded in the calculational method used and the inaccuracies encountered in the database and/or modeling. The standard deviation in the quantity u_i is given by $\sigma_i = \sigma_{ir}(c_i/e_i)$ where σ_{ir} is the relative standard deviation obtained from the relation $\sigma_{ir}^2 = \sigma_{cir}^2 + \sigma_{eir}^2$ in which σ_{cir}^2 and σ_{eir}^2 are the relative standard deviations in c_i and e_i respectively. The extremes around the mean value u_i are given by $u_{i\max} = u_i + \sigma_i$ and $u_{i\min} = u_i - \sigma_i$.

Suppose we divide the space of the prediction uncertainty u into intervals Δu, and ask what fraction of experiments among the total number of experiments N has a prediction uncertainty in any particular interval. The normalized density function (NDF) $f(u)$ is obtained such that the quantity $Nf(u)\,\Delta u$ is the number of experiments whose prediction uncertainty u in the response R is within the interval between u and $u + \Delta u$. The NDF $f(u)$ is thus an histogram which could approach a smooth curve as $N \to \infty$ and $\Delta u = \mathrm{d}u \to 0$. In this case, the mean value $\bar{u}$ of the prediction uncertainty in the response R among all the experiments considered is evaluated from

$$\bar{u} = \int_{-1}^{\infty} uf(u)\,\mathrm{d}u \tag{1}$$

and the normalization condition is given by

$$\int_{-1}^{+\infty} f(u)\,\mathrm{d}u = 1 \tag{2}$$

The lower boundary of $u = (c/e) - 1$ is -1 (when $c = 0$) and the upper boundary is ∞ (when $c \to \infty$). In practice, however, the total number of experiments N is limited and a finite interval width Δu is used. The mean prediction uncertainty $\bar{u}$ is thus obtained from $\bar{u} = \sum_{j=1}^{j=K} uf_j$ and the normalization condition is given by $\sum_{j=1}^{j=K} f_j = 1$, where K is the total number of intervals j of a width Δu_j considered between predetermined upper and lower bounds $U(\max)$ and $U(\min)$, and the quantity Nf_j is the number of experiments whose prediction uncertainty in the response R lies within the uncertainty interval boundaries u_j and $u_j + \Delta u_j$. The standard deviation σ_u is defined as

$$\sigma_u = \left[\sum_{j=1}^{j=K} (u - \bar{u})^2 f_j\right]^{1/2} \tag{3}$$

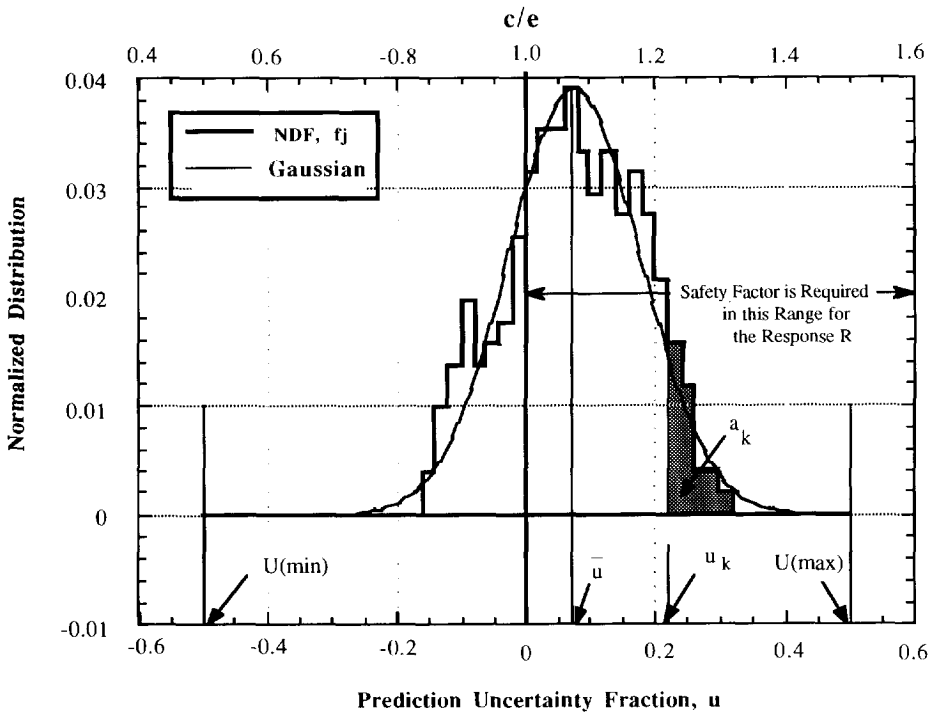

Fig. 1. Example of a normalized density function f_j for a nuclear response R where a design safety factor is required.

Fig. 1 shows an example of a possible NDF f_j for a nuclear response R (in the figure, u is presented in fraction). Also shown is a Gaussian density function that has the same mean $\bar{u}$ and the same standard deviation σ_u. The area under both distributions is unity. The resemblance between the two distribution could improve as the number of experiments considered increases.

According to Fig. 1, it is most likely that calculated value c of the response R will exceed the measured value e, since the mean value $\bar{u}$ is positive. However, there is a definite probability that c could also be smaller than e. For a blanket/shield designer who would like to account for the prediction uncertainties encountered in integral experiments in his design, the seriousness and impact of the fact that the calculated value c could be either larger or smaller than the actual measured value e depends on the nuclear response in hand. For the TPR, if c is larger than e, then the calculations over predict the tritium production in the blanket and the tritium breeding ratio (TBR) may fall below a threshold value which ensures the condition for tritium self-sufficiency to be met. In this case, designers should apply a safety factor to the calculated TPR. To derive this factor from the constructed NDF, one can notice from Fig. 1 that the probability that the uncertainty in the calculated response R could be larger than a given value u_k is expressed by the shaded area a_k. By dividing the calculated TPR by a correction factor, $S_k = u_k + 1 = c_k/e_k$, in order to bring calculations into agreement with measurements (e.g. $c_k/e_k = 1$), we are accepting a risk level (RL), quantified by the quantity a_k, the calculations could still be larger than measurements (i.e. the confidence level (CL) that the calculated TPR will exceed the measured value by no more than u_k is given by the fraciton $(1 - a_k)$). In this case, the correction (safety) factor chosen is S_k. Using larger safety factors implies that more conservatism is applied to the design and that a higher confidence level is achieved in calculating the response in hand.

The response considered in the present work is the line-integrated TPR from Li-6 (T_6) and Li-7 (T_7). In each experiment i, the prediction uncertainty u_i and standard deviation σ_i were derived independently for the line-integrated T_6 and T_7 from local values at several locations j inside the test assembly. The procedures applied are as follows [4]. (a) Using the calculation data set $\{z_j, c_j, \sigma_{cj}^2\}$, where the z_j are the measuring

locations, c_j are the data values at locations z_j and σ_{cj}^2 are the variance of the data values at locations z_j, find the curve that can best fit the data c_j (using least square fitting). The variance (and covariance) of the coefficients of the fitting curve are derived from the variances (uncertainties) σ_{ci}^2. (b) Perform line-integration of the fitting curve between the breeding zone boundaries, $Z1$ and $Z2$. The integration yields the value C and its variance σ_C^2. (c) Likewise, using the experimental data set $\{z_j, e_j, \sigma_{ej}^2\}$, perform the above procedures to obtain the integrated value E, and its variance σ_E^2. (d) The prediction uncertainty in the integrated TPR is quantified in terms of $u_i = C/E - 1$ whose variance σ_i^2 is derived from the variances σ_C^2 and σ_E^2.

In each experiment i, the prediction uncertainty in TPR from natural lithium (T_n), denoted, $u_n = C_n/E_n - 1$, can be obtained from the prediction uncertainty in the line-integrated T_6, u_6, and T_7, u_7 by applying the following equations:

$$C_n = \alpha_6 C_6 + \alpha_7 C_7 \qquad E_n = \alpha_6 E_6 + \alpha_7 E_7 \tag{4}$$

$$\sigma_{C_n}^2 = \alpha_6^2 \sigma_{C_6}^2 + \alpha_7^2 \sigma_{C_7}^2 \qquad \sigma_{E_n}^2 = \alpha_6^2 \sigma_{E_6}^2 + \alpha_7^2 \sigma_{E_7}^2 \tag{5}$$

$$\sigma_{nr}^2 = \sigma_{C_{nr}}^2 + \sigma_{E_{nr}}^2 \tag{6}$$

$$\sigma_{C_{nr}}^2 = \sigma_{C_n}^2 / C_n^2 \qquad \sigma_{E_{nr}}^2 = \sigma_{E_n}^2 / E_n^2 \tag{7}$$

where α_6 and α_7 are the enrichment of Li-6 (0.0742) and Li-7 (0.9258) in natural lithium and $\sigma_{C_6}^2$ and $\sigma_{C_7}^2$ are the variances in the integrated values C_6 and C_7. Likewise, the variances in the integrated values E_6, and E_7 are $\sigma_{E_6}^2$ and $\sigma_{E_7}^2$. The quantity σ_{nr}^2 is the relative variance of the calculated-to-experimental value C_n/E_n.

3. Description of the experiments

Numerous experiments were performed at the Fusion Neutronics Source (FNS) facility at JAERI during the USDOE/JAERI Collaboration. Phase I experiments were performed in an open geometry with a 14 MeV point source. The test assembly is a cylinder of diameter $D = 60$ cm and length $L = 61$ cm constructed from Li_2O blocks. Three categories of experiment were conducted: (a) the reference experiment, P1-REF; (b) first wall experiment, P1-WFW-0.5 (a 0.5 cm thick stainless steel first wall (316SS) was placed in front of the Li_2O assembly) and P1-WFW-1.5; (c) beryllium experiments in which 5 cm thick Be, 10 cm thick Be, and 5 cm thick Li_2O + 5 cm thick Be layers were placed in front of the Li_2O assembly separately, designated P1-WBE in the present work. Details of the measurements and analysis performed in this phase can be found in Refs. [5,6].

Phase II experiments were also performed with a point source. The test assembly is a rectangular shape of dimensions 86.4 cm × 86.4 cm × 60.71 cm placed at one end of a rectangular enclosure made of Li_2CO_3; the D–T neutron source was placed inside the cavity at a distance of about 78 cm from the square front surface of the test assembly. Three experiments were performed in Phase IIA: (a) the reference (P2A-REF) experiment, (b) the beryllium front (P2A-BEF) experiment; (c) the Be sandwich (P2A-BES) experiment. The thickness of the Be layer was 5 cm. The experiments performed in Phase IIB were similar except that the inner surface of the Li_2CO_3 enclosure was covered by a 5 cm thick Be layer. Three experiments were performed in this phase, namely the reference (P2B-REF) experiment, the Be front (P2B-BEF) experiment, and the Be front with 0.5 cm thick FW (P2B-BEFWFW) experiment. Details of the measurements and analysis for Phases IIA and IIB can be found in Refs. [7–12]. In Phase IIC, two experiments were performed on the heterogeneity effects on the TPR, namely, the water coolant channel (P2C-WCC) experiment and the multilayer beryllium edge-on experiment (P2C-BEO) [13–17].

In Phase III, an annular test assembly with an inner square cavity of dimensions 42.55 cm × 42.55 cm surrounded the point source and was moved periodically back and forth in the axial direction ($z = -100$ cm to $z = 100$ cm) relative to the source and hence a simulated line source was created at the central axis of the cavity. The reference experiment of phase IIIA has a 1.5 cm thick 304 SS first wall followed by a 20 cm thick Li_2O zone and a 20 cm thick Li_2CO_3 zone with an approximately 2 cm thick polyethylene (PE) outer layer. Three radial drawers (A, B, and C at $z = -53$ cm, 2.53 cm, and 48.4 cm respectively) were installed through which measurements were taken. In Phase IIIB, a 2.54 cm thick carbon layer was added at the inner surface of the cavity to act as an armor zone. Fig. 2 shows the geometrical arrangement of this experiment. In Phase IIIC, a squared opening of 455.5 × 455.5 mm^2 was made at the center of the Phase IIIB system. Measurements of the TPR were taken at the three drawers (A, B, and C) facing the large opening and along a radial drawer D adjacent to the opening itself. More details on Phase III experiments can be found in Refs. [18–23]. Table 1 summarizes all the experiments considered in the present study. In some of these experiments, the predicted uncertainty in the line-integrated TPR was calculated separately in several sub-zones inside the breeding zone. For example, in the beryllium sandwich experiment of Phase IIA (P2A-BES), two sub-zones were considered (zone 1 in front

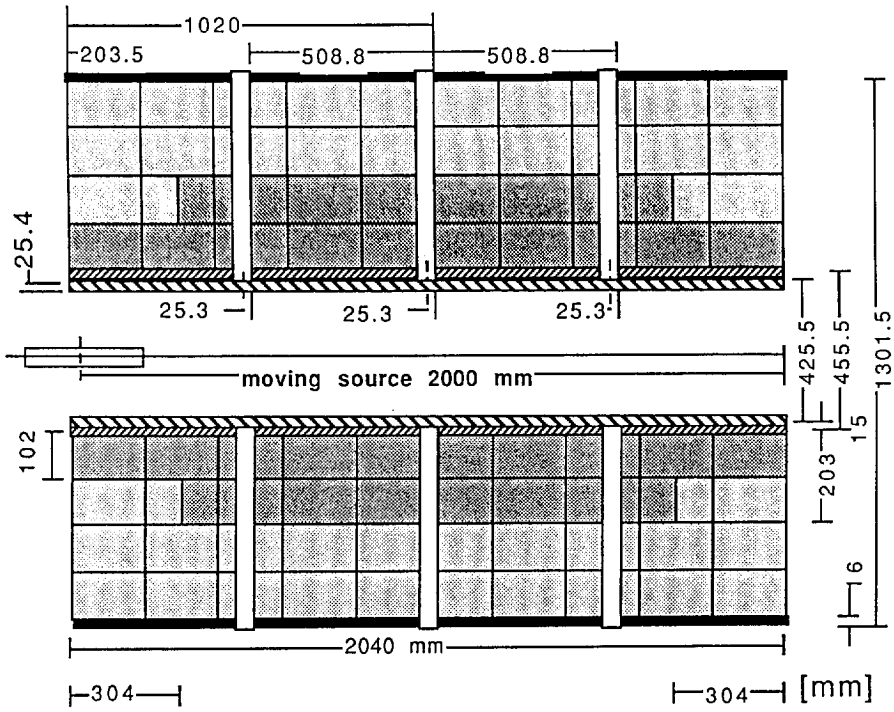

(a)

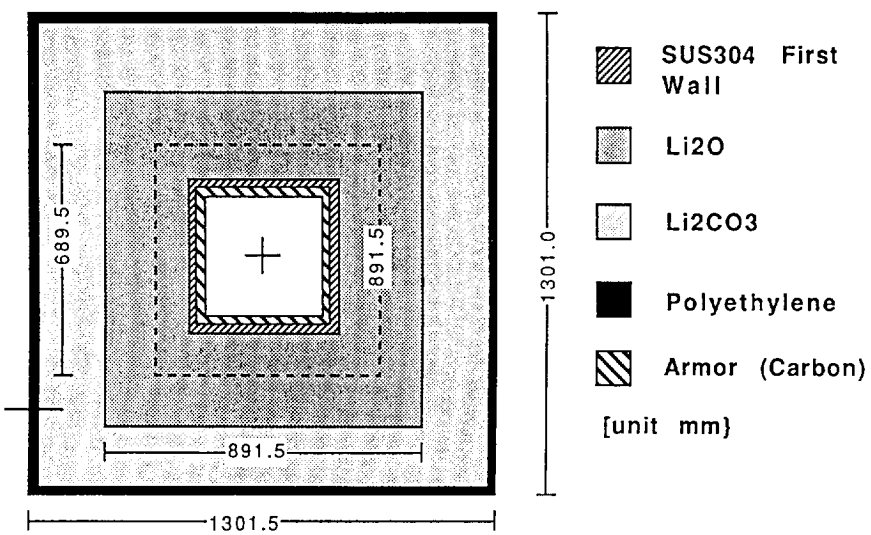

(b)

Fig. 2. The geometrical arrangement of the phase IIIB experiment with the simulated line source: (a) elevation, (b) cross-section.

of the Be layer and zone 2 behind it). Five sub-zones (1–5) were considered in the water coolant channel experiment of Phase IIC (P2C-WCC) whose boundaries are described in Ref. [16]. Additionally, in the experiment (case) labeled P3A-All, the experimental and the calculational data sets in the three drawers A, B, and C were combined to give an overall profile of the TPR averaged over the three drawers.

4. Calculational methods

In the US calculations, the MCNP code [24], version 3A, was used in analyzing phase I and IIA experiments with the Monte Carlo (MC) method while version 3B was applied in analyzing subsequent experiments. The pointwise continuous energy/angle cross-section library RMCCS/BMCCS (ENDF/B-V, version 2) was used. The DOT4.3 [25] and DOT5.1 codes were used in the two-dimensional S_n discrete ordinates (DO) treatment along with the first collision code RUFF [26]. The MATXS6 library [27] (ENDF/B-V, version 2, 80-g) was used (P5-S16) for Phase I–II and the MATXS5 (ENDF/B-V, version 2, 30-g) was applied (P3-S16) in Phase III analysis. The beryllium data of LANL [28] were used in the US analysis.

The MORSE-DD [29] code was used by JAERI in the MC calculations and it utilizes the double differential cross-section library DDL/J3P1 (125 neutron group) based on JENDL3/PR1 data file. In some cases, the GMVP code [30] was also used to re-analyze some experiments, particularly in Phase III with JENDL3/PR2 data. The FSXJP7 library (P_7, 125-g) was applied in JAERI's calculations with DOT3.5/GRTUNCL codes and is based on JENDL3/PR2. In folding the NE213 experimental data to obtain measured values for T_7, the JENDL3/PR2 data for the ^{7}Li(n,n'α)t cross-section were used.

5. Results and discussion

The prediction uncertainty u_i in the line-integrated T_6 and T_7 based on the discrete ordinates (DO) and Monte Carlo (MC) calculations along with the associated standard deviations $\pm\sigma_i$ were obtained in each experiment i according to the procedures described in Section 2. The calculational uncertainties in the MC calculations are those arising from the statistical treatment. In the discrete ordinate case, the deviations σ_i include the experimental errors only. No account was made in the calculational errors of the contribution arising from nuclear data uncertainties. In this regard, previous work has indicated that the uncertainties in local T_6 and T_7 due to uncertainties in nuclear data are 2%–4% and 4%–6% respectively [31]. These uncertainties could be larger (by 9%) when the uncertainties in the secondary energy distribution (SED) are accounted for [32]. It should be noted that the uncertainties in the integrated TBR in several candidate blanket concepts due to data uncertainties were found to be 2%–5% [2]. In addition, and with regard to the DO method, other sources of uncertainties in the calculated TPR such as the number of energy group considered, the size of the spatial mesh, the quadrature set and the order of the Legendre polynomials used to describe the cross-section data. Recent analysis [33,34] has indicated that the discrepancies between results based on coarse group vs. fine group could be as large as about 20%. Likewise, a coarse spatial mesh influences the low-energy neutron flux by about 20% at maximum. Other discretization parameters have a small influence of 1%–2%. However, results from a low number of histories (about 10^4) in the MC calculations can deviate from results based on a large number of histories (about 10^8) by as much as 80% [34]. The results reported here, however, are based on fine group/mesh/quadrature sets in the DO method and for a large number of histories in the MC calculations.

Some of the experimental errors were not readily available at some locations in some of the experiments. In these cases, an experimental error of approximately 3.5% was assumed in the Li-glass measurements and approximately 6.5% in the NE213 measurements.

5.1. Line-integrated tritium production rate from Li-6 (T_6)

Fig. 3 shows the prediction uncertainty in the line-integrated T_6, as obtained by the US, based on Li-glass measurements. The counterpart uncertainties based on JAERI's calculations are shown in Fig. 4. Fig. 5 shows the histogram of the NDF of the prediction uncertainty u, based on all the discrete ordinates and MC cases shown in Fig. 3 (i.e. no distinction is made among calculational methods), in addition to the NDF in the case where the experimental errors E are ignored while accounting only for the calculational C errors in estimating σ_i. The contribution to σ_i from the calculational errors is represented by the black bars in Figs. 3 and 4. The Gaussian curves that have the same mean prediction uncertainty $\bar{u}$ and deviation σ_u as those of the NDFs are also shown in Fig. 5 for comparison. The Gaussian curves give close representations of the NDFs, particularly in the case when the calculational and experimental (C,E) errors are included.

The NDFs based on JAERI's cases given in Fig. 4 are depicted in Fig. 6. Comparing the Gaussian curves that approximate the NDFs, the mean prediction uncertainty $\bar{u}$ is lower than that obtained by the US by about 3%. Fig. 7 shows the NDF for the prediction uncertainty u constructed from all the cases shown in Figs. 3 and 4 (denoted US&JAERI in subsequent figures).

Table 1
Abbreviations for the experiments conducted in Phase I through Phase III

Phase	Experiment or case	Abbreviation
I	Reference experiment	P1-REF
I	First wall experiment, FW of 0.5 cm	P1-WFW(0.5)
I	First wall experiment, FW of 1.5 cm	P1-WFW(1.5)
I	Beryllium experiment, Be 5 cm	P1-WBE(5 cm)
I	Beryllium experiment, Be 10 cm	P1-WBE(10 cm)
IIA	Reference experiment	P2A-REF
IIA	Beryllium front experiment	P2A-BEF
IIA	Beryllium-sandwich experiment	P-2ABES
IIB	Reference experiment	P2B-REF
IIB	Beryllium front experiment	P2B-BEF
IIB	Beryllium front with first wall experiment	P2B-BEFWFW
IIC	Water coolant channel experiment	P2C-WCC
IIC	Beryllium edge-on experiment	P2C-BEO
IIIA	Reference experiment, drawer A	P3A-DA
IIIA	Reference experiment, drawer B	P3A-BD
IIIA	Reference experiment, drawer C	P3A-DC
IIIA	Reference experiment, drawer A, B, C	P3A-All
IIIB	Armor experiment, drawer A	P3B-DA
IIIB	Armor experiment, drawer B	P3B-DB
IIIB	Armor experiment, drawer C	P3B-DC
IIIB	Armor experiment, drawer A, B, C	P3B-All
IIIC	Large opening experiment, drawer A	P3C-DA
IIIC	Large opening experiment, drawer B	P3C-DB
IIIC	Large opening experiment, drawer C	P3C-DC
IIIC	Large opening experiment, drawer D	P3C-DD
IIIC	Large opening experiment, drawer A, B, C	P3C-All

Table 2 gives the mean uncertainty $\bar{u}$, the standard deviation σ_u, the root mean square value u_{rms}, and the most probable value u_{mp}, as obtained from the NDFs (not the Gaussians). Note that $\sigma_u = (u_{\text{rms}}^2 - \bar{u}^2)^{1/2}$. The most probable value u_{mp} is defined as the value of u at which the NDF has its largest value. When the calculational and experimental errors are considered, the mean uncertainty in T_6 is positive. This reflects that calculations performed by blanket designers are likely to be larger than the actual measured values, emphasizing the need to apply safety factors. Although the mean uncertainty $\bar{u}$ is relatively small (US approximately 3%, JAERI less than 1%), the spread around the mean value σ_u is large (US approximately 9%, JAERI approximately 8%; less than in the US case). When all the cases shown in Figs. 3 and 4 are considered, the values of $\bar{u}$ and σ_u fall between those of the US and JAERI.

The relationship between the chosen safety factor S_k ($S_k = u_k + 1 = C/E$) and the associated confidence level $(\text{CL})_k$ in percentage, is shown in Fig. 8 (the C and E errors are included). The labels US, JAERI, and US&JAERI denote that the curves are obtained from the NDFs given in Fig. 5, Fig. 6 and Fig. 7 respectively, according to the procedures described in Section 2. If no safety factor is used ($S_k = 1 = C/E$), the confidence level that calculated T_6 will not exceed the actual measured value is about 38% in the US case and about 46% in JAERI's case. To have 100% confidence, the safety factor to be used is 1.30 in the US case and 1.20 in JAERI's case. (Statistically, no such 100% confidence can be achieved since there are uncertainties in the curves shown in Fig. 8 themselves owing to the limited number of cases considered n, of magnitude approximately $1/n^{1/2}$. The factors 1.3 and 1.2 can be viewed as the largest value of C/E as evidenced from the analysis of all experiments, considering both the experimental and calculational errors. They can also be viewed as the most conservative correction and safety factors.) Thus, for the same confidence level, the required safety factors are larger in the US case than in JAERI's case. Their values, however, assume the average between the two cases when the NDF constructed from all cases shown in Figs. 3 and 4 is used to derive the $(\text{CL})_k - S_k$ curve.

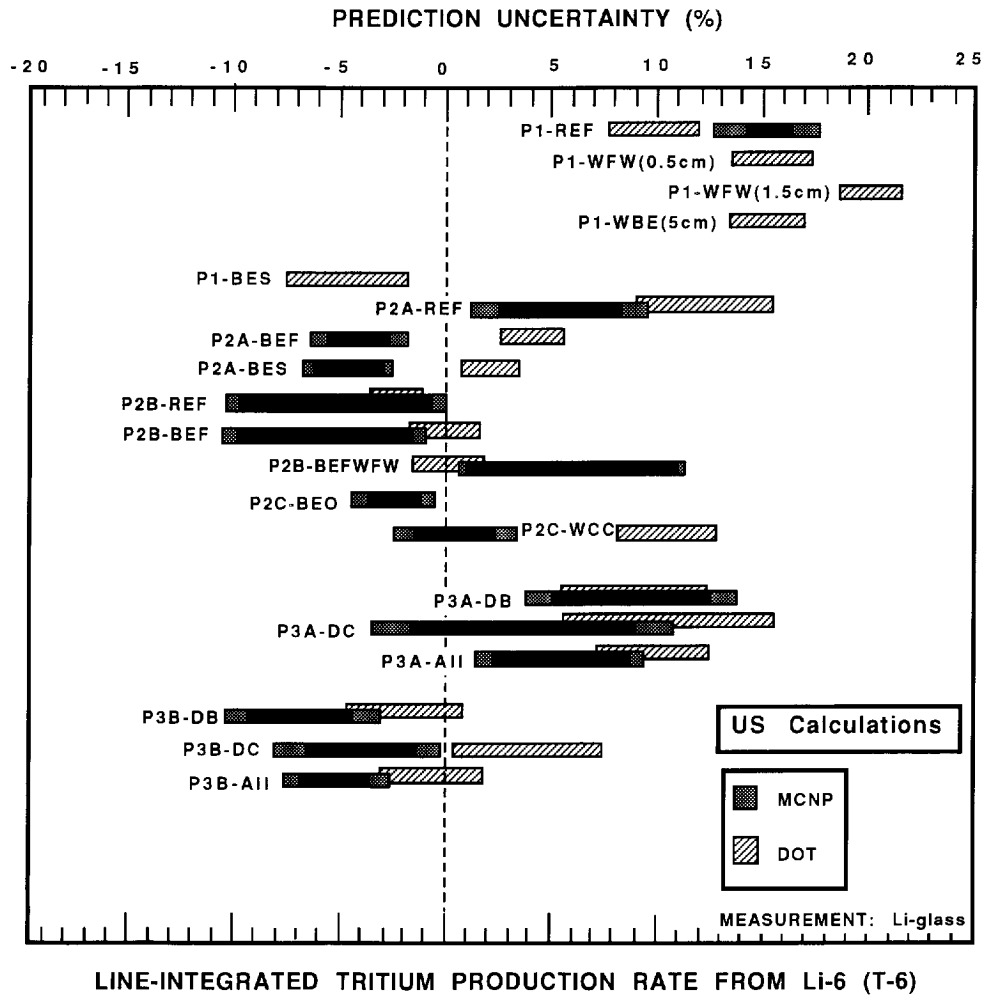

Fig. 3. The prediction uncertainty in the line-integrated tritium production rate from Li-6 (T_6) (US calculations, Li-glass measurements).

Effect of calculational methods applied

Distinction was made between the discrete ordinates (DO) and Monte Carlo (MC) calculational methods in evaluating the required safety factors. Figs. 9 and 10 show the NDFs and the approximating Gaussian curves from the DO and MC methods used by the US and JAERI respectively. The required safety factors as a function of the assigned confidence levels are shown in Fig. 11 based on the US, JAERI and US&JAERI calculations. Table 3 gives the relevant statistical parameters ($\bar{u}$, σ_u, etc) of these distributions when each calculational method is considered separately. The safety factors are summarized in Table 4 for several confidence levels. Also given are the safety factors when the cases based on the two calculational methods are treated together.

Based on the US calculations, the mean values $\bar{u}$ of T_6 based on the DO and MC method are about 7.6% and 0.8% respectively (as opposed to about 3% when both methods are considered together) with spreads σ_u of about 7.7% and 7.6%, indicating that the DO method tends to give larger T_6 by approximately 8% than the results based on the MC method. This is also true for the safety factors at other confidence levels,

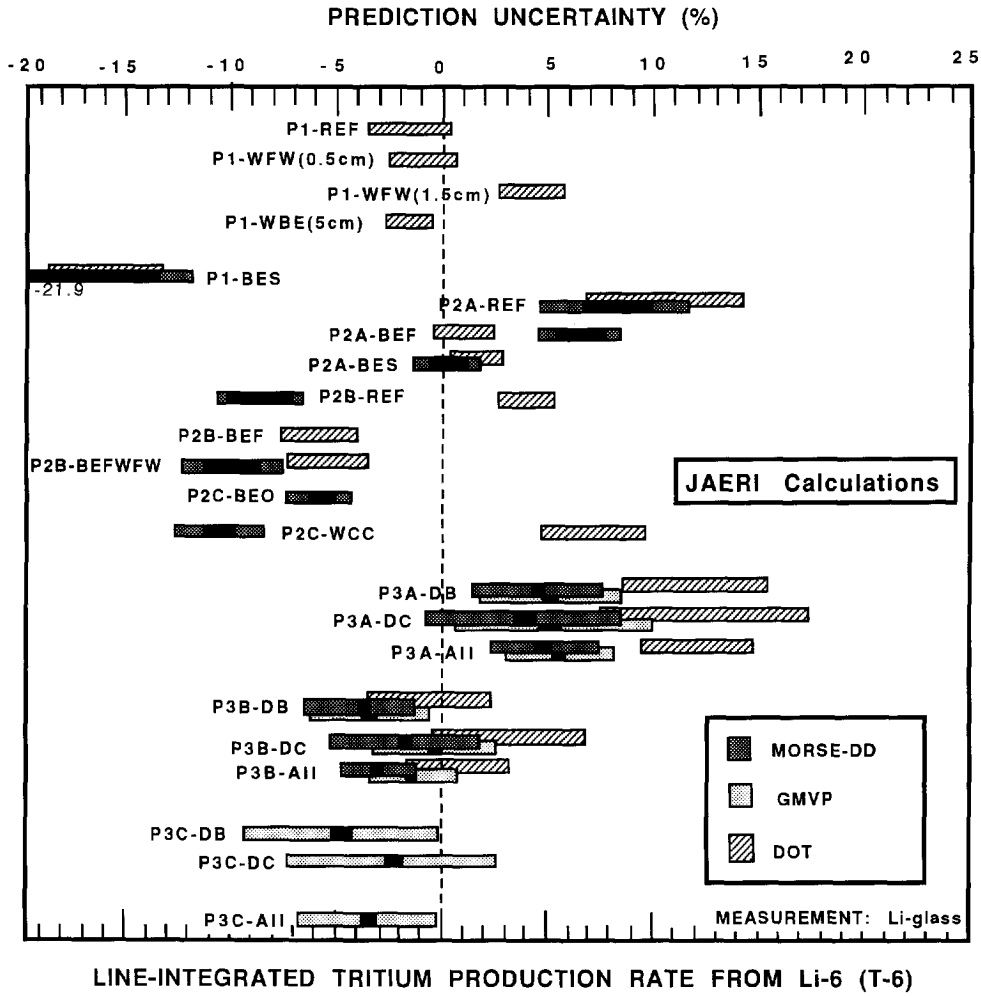

Fig. 4. The prediction uncertainty in the line-integrated tritium production rate from Li-6 (T_6) (JAERI's calculations, Li-glass measurements).

which are 7%–8% larger in the DO case as compared with the MC case. In JAERI's case, $\bar{u}$ is approximately 3.6% and −2.5% (as opposed to about 0.2% when both methods are considered together), with spreads of about 7% and 7.4% around the mean value in the DO and MC cases respectively. This again indicates that the DO method gives a larger prediction uncertainty (and safety factor) by about 6%. In both methods, the mean prediction uncertainty $\bar{u}$ based on the US calculations is larger than JAERI's by 2%–4%. The spread around the mean uncertainty is also slightly larger (by less than 1%) in the US case than in JAERI's case. The required safety factors are also larger by about 4%–5% (see Table 4).

5.2. Line-integrated tritium production rate from Li-7 (T_7)

The prediction uncertainty in the line-integrated T_7 u_i and the associated standard deviation $\pm\sigma_i$ in each experiment (case) i are shown in Figs. 12 and 13 as obtained by the US and JAERI respectively, using the NE213 method. The $\pm\sigma_i$ are generally larger than those of T_6 shown in Figs. 3 and 4 and the uncertainty tends to have negative values as we proceed from Phase I to Phase III. The calculational errors of the MC calculations (respresented by the black bars) are small as obtained from the GMVP code (JAERI) compared with those encountered in the MORSE-DD and MCNP

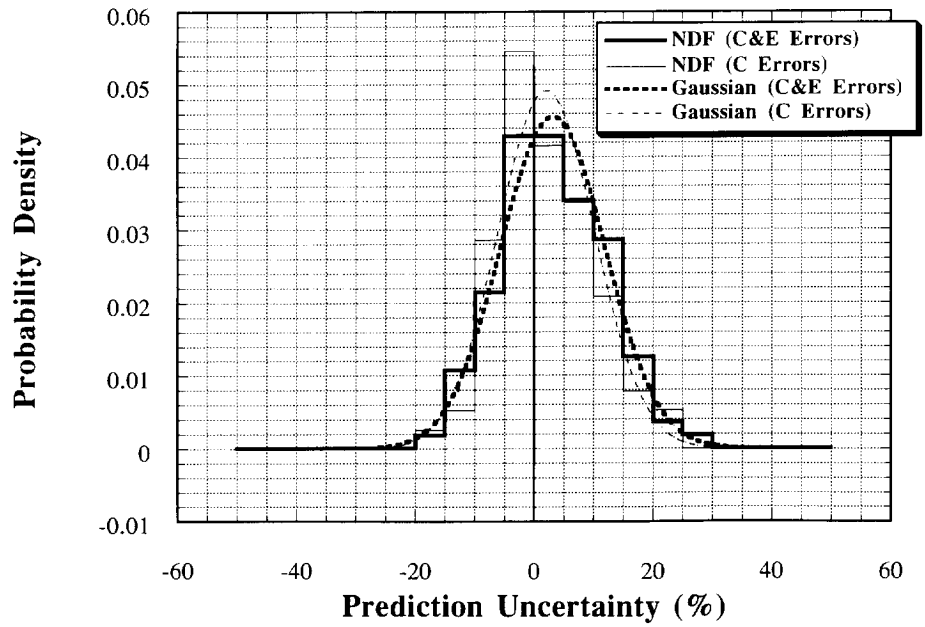

Fig. 5. Normalized density function f_j of the prediction uncertainty of T_6 (US codes and data, Li-glass measurements, all phases).

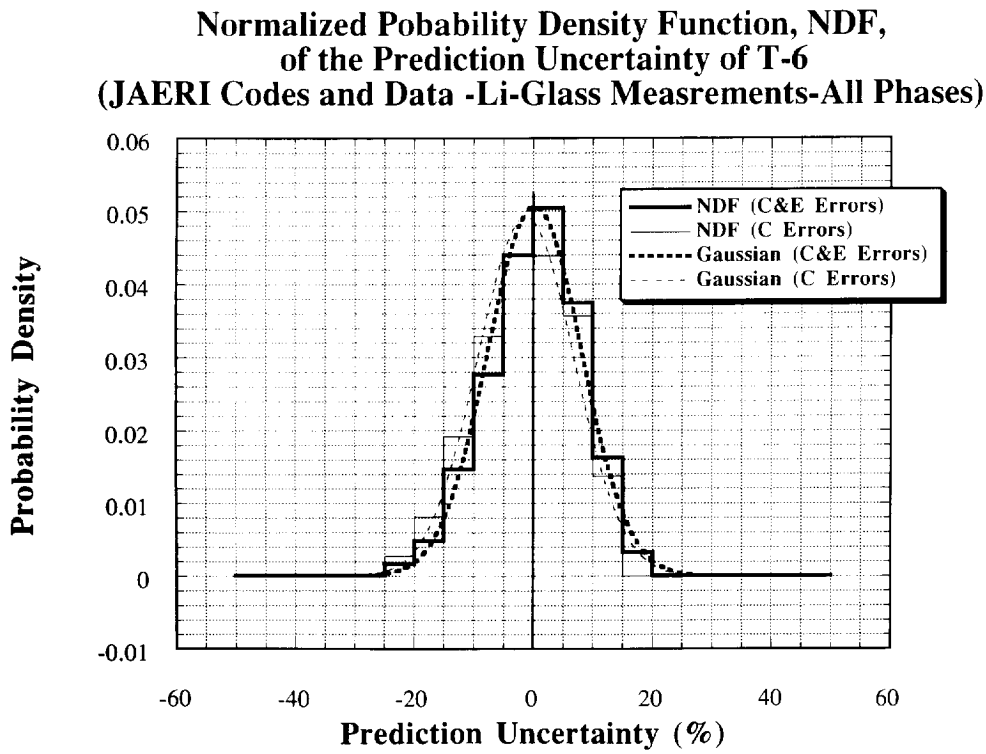

Fig. 6. Normalized density function f_j of the prediction uncertainty of T_6 (JAERI's codes and data, Li-glass measurements, all phases).

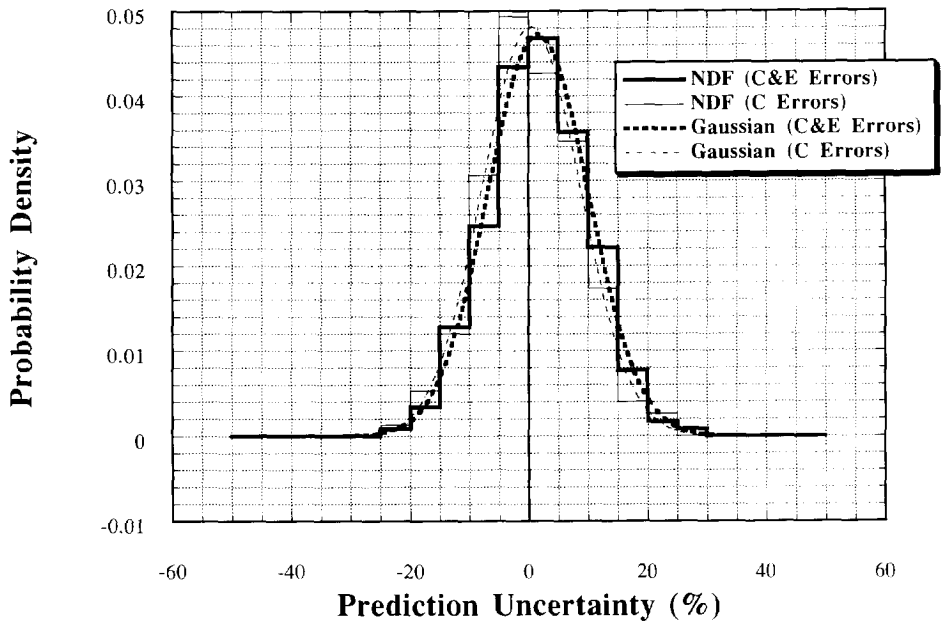

Fig. 7. Normalized density function f_j of the prediction uncertainty of T_6 (US&JAERI codes and data, Li-glass measurements, all phases).

Table 2
Statistical parameters of the prediction uncertainty u (%) of the line-integrated tritium production rate from Li-6 (T_6), Li-7 (T_7), and Li-n (T_n) as obtained from various calculational and experimental methods

Method	Calculational and experimental error included			Calculational errors only included		
	US	JAERI	US&JAERI	US	JAERI	US&JAERI
T_6 (Li-glass)						
Number of cases considered	50	58	108	50	58	108
$\bar{u}$ (average)	3.17	0.22	1.63	2.05	−1.27	0.43
σ_u (standard deviation)	8.75	7.87	8.43	8.11	8.09	8.27
u_{rms} (root mean square)	9.31	7.87	8.58	8.36	8.19	8.28
u_{mp} (most probable)	0	2.5	2.5	−2.5	0	−2.5
T_7 (NE213)						
Number of cases considered	49	56	105	49	56	105
$\bar{u}$ (average)	7.58	−1.99	2.69	5.0	−3.47	1.14
σ_u (standard deviation)	10.54	7.28	10.21	9.91	7.23	9.75
u_{rms} (root mean square)	12.98	7.55	10.56	11.09	8.02	9.81
u_{mp} (most probable)	7.50	−7.50	2.5	5.0	−10.0	2.5
T_n (T_6(Li-glass) + T_7(NE213))						
Number of cases considered	33	38	71	33	38	71
$\bar{u}$ (average)	3.33	−2.36	0.40	2.74	−2.63	0.12
σ_u (standard deviation)	7.76	6.09	7.51	7.63	6.47	7.58
u_{rms} (root mean square)	8.45	6.53	7.52	8.11	6.98	7.58
u_{mp} (most probable)	2.5	−2.5	−2.5	−2.5	−7.5	−7.5

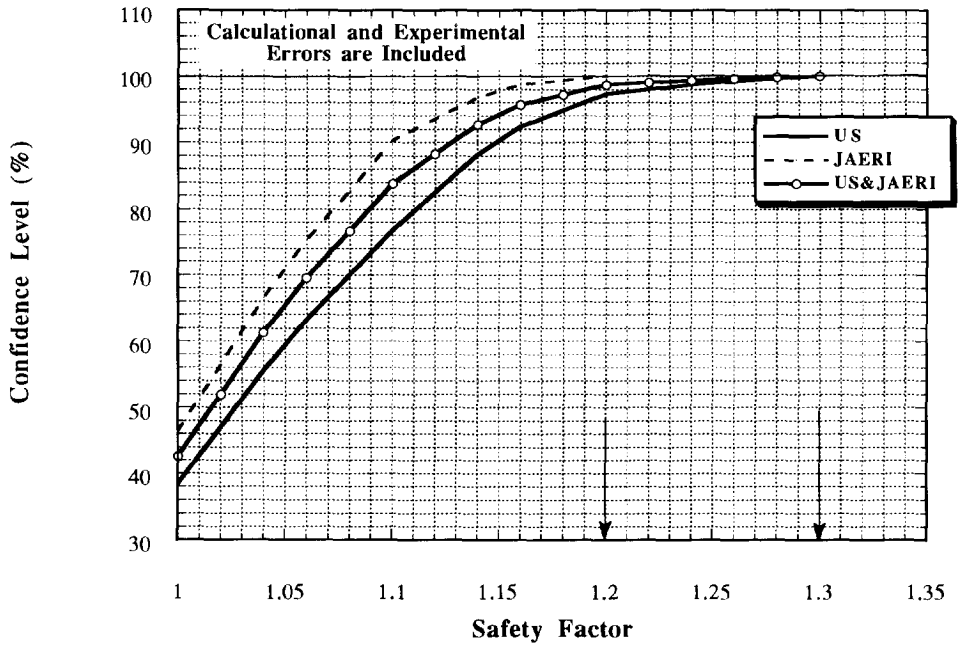

Fig. 8. Confidence level for calculations not to exceed measurements as a function of design safety factors for T_6 (all phases, Li-glass measurements, C and E errors are included).

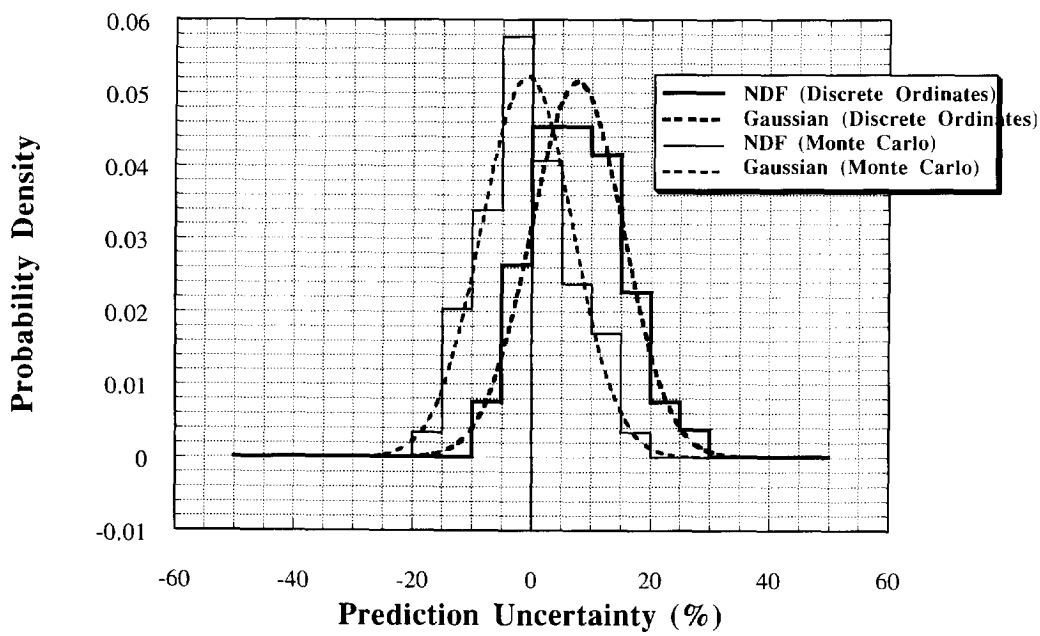

Fig. 9. The normalized density function of the prediction uncertainty in T_6 with distinction between calculational method (US calculations, Li-glass measurements, all phases).

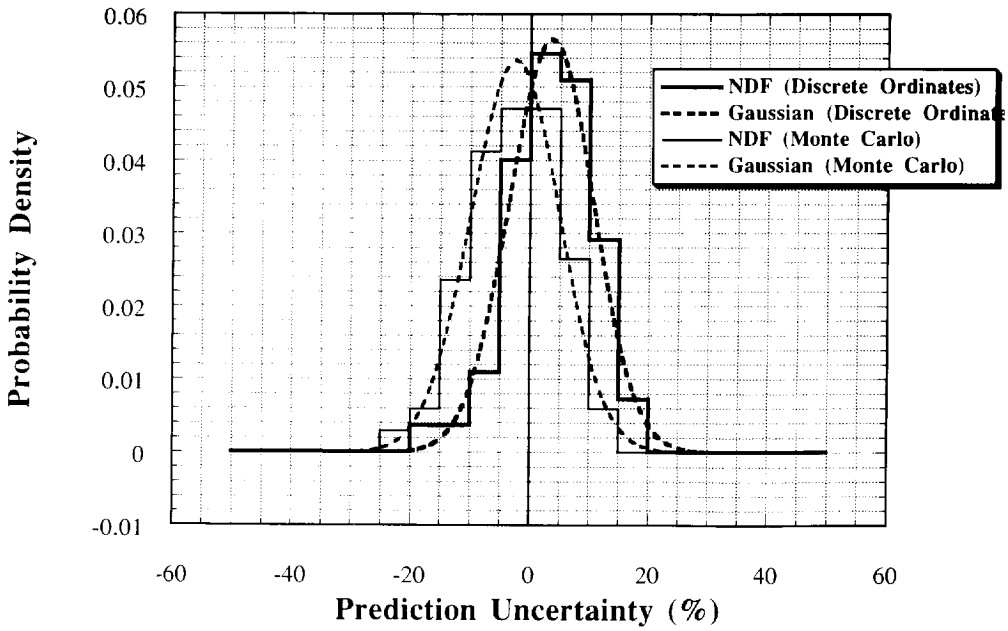

Fig. 10. The normalized density function of the prediction uncertainty in T_6 with distinction between calculational method (JAERI calculations, Li-glass measurements, all phases).

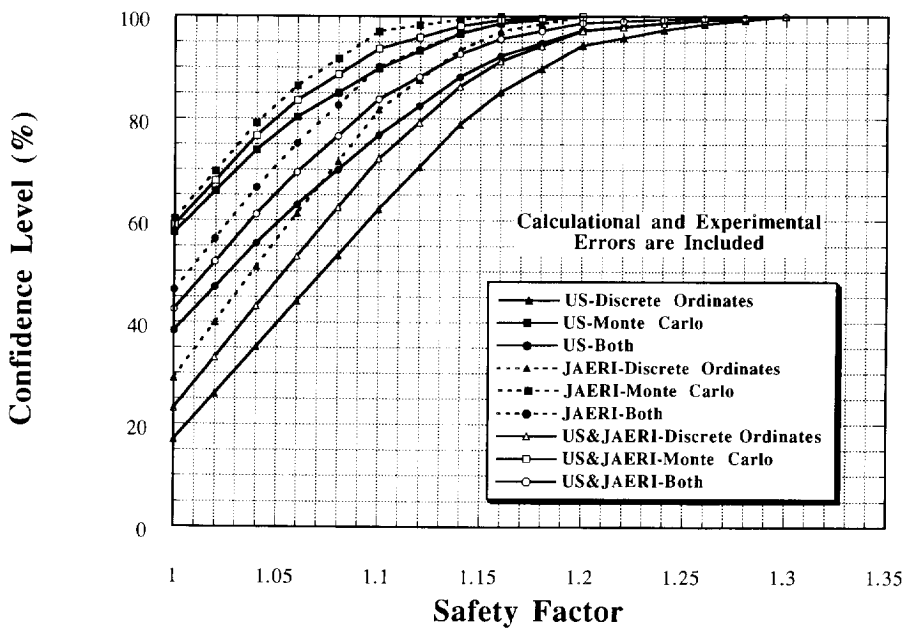

Fig. 11. Confidence level for calculations not to exceed measurements as a function of design safety factors for T_6 (Li-glass measurements, all phases).

Table 3
Statistical parameters of the prediction uncertainty, u (%) of tritium production rate as obtained from various calculational methods

Method	Discrete ordinates method			Monte Carlo method		
	US	JAERI	US&JAERI	US	JAERI	US&JAERI
T_6 (Li-glass)						
Number of cases considered	26	26	52	24	32	56
$\bar{u}$ (average)	7.59	3.59	5.56	−0.81	−2.50	−1.71
σ_u (standard deviation)	7.74	7.05	7.66	7.63	7.43	7.57
u_{rms} (root mean square)	10.84	7.91	9.46	7.67	7.84	7.76
u_{mp} (most probable)	5.00	2.5	2.5	−2.5	0.0	−2.5
Design safety factor (100% confidence) [a]	1.30	1.2	1.30	1.2	1.16	1.20
T_7 (NE213)						
Number of cases considered	26	26	52	23	30	53
$\bar{u}$ (average)	10.30	−1.12	4.64	4.81	−2.78	0.82
σ_u (standard deviation)	10.45	6.53	10.43	9.89	7.81	9.63
u_{rms} (root mean square)	14.67	6.63	11.41	10.99	8.29	9.67
u_{mp} (most probable)	7.70	−2.5	2.50	5.00	−7.50	2.50
Design safety factor (100% confidence)	1.30	1.10	1.30	1.35	1.16	1.35
T_n (T_6(Li-glass) + T_7(NE213))						
Number of cases considered	18	18	36	15	20	35
$\bar{u}$ (average)	5.69	−0.24	2.95	0.50	−4.00	−2.07
σ_u (standard deviation)	7.56	6.33	7.62	7.02	5.33	6.52
u_{rms} (root mean square)	9.46	6.33	8.17	7.04	6.69	6.84
u_{mp} (most probable)	2.5	2.50	2.50	2.50	−2.50	−2.50
Design safety factor (100% confidence)	1.26	1.16	1.26	1.20	1.10	1.20

[a] Statistically, no such 100% confidence can be achieved (see text). These factors can be viewed as the largest values of C/E as evidenced from the analysis of all experiments, considering both the experimental and calculational errors.

calculations. The Gaussian distributions that approximate the NDFs are shown in Figs. 14 and 15 (considering the DO and MC cases together). Table 2 gives the relevant statistical parameters of the prediction uncertainty estimated from the respective NDFs.

The uncertainty $\bar{u}$ is negative in JAERI's calculation ($\bar{u} \approx -2\%$) while it is positive ($\bar{u} \approx 7.6\%$) in the US calculations. The mean prediction uncertainty in the US calculations is larger than JAERI's by about 9%. The NDF are wider in the US case ($\pm\sigma_u \approx 11\%$) and the spread σ_u is larger than in JAERI's case by about 3%–4%.

Effect of calculational methods applied

Figs. 16 and 17 show the NDFs and the approximating Gaussian curves when the DO and MC cases are treated separately based on the US and JAERI calculations respectively. The required safety factors as a function of the assigned confidence levels are shown in Fig. 18. Table 3 also gives the statistical parameters ($\bar{u}$, σ_u, etc) obtained from the constructed NDFs and the required safety factors are summarized in Table 4 for several confidence levels. As shown for the combined case of DO and MC (denoted "both" in Figs. 11 and 18), if no safety factors are used ($S_k = 1$), the confidence level in the US calculations is about 24%, and about 60% in JAERI's calculations. When results from the US and JAERI are combined, the values of these levels are between those of the US and JAERI. The most conservative safety factors are 1.35 (US) and 1.16 (JAERI).

Based on the US calculations, the mean values $\bar{u}$ of T_7 from the DO and MC methods are approximately 10.3% and 4.8% respectively (as opposed to about 7.6%

Table 4
Design safety factors for tritium production rate as a function of the required confidence level (based on results from the US/JAERI collaborative program on fusion blanket neutronics)

Level of confidence (%)	Tritium production from lithium-6 (T_6), Li-glass measurement			Tritium production from lithium-7 (T_7), NE213 measurements			Tritium production from lithium-n (T_n), combined method		
	US	JAERI	US&JAERI	US	JAERI	US&JAERI	US	JAERI	US&JAERI
50	1.02 [a]	1.00	1.00	1.09	1.00	1.02	1.03	1.00	1.00
	1.07 [b]	1.03	1.05	1.11	1.00	1.04	1.04	1.00	1.02
	1.00 [c]	1.00	1.00	1.04	1.00	1.01	1.00	1.00	1.00
80	1.11	1.07	1.09	1.17	1.05	1.11	1.11	1.03	1.07
	1.14	1.10	1.12	1.20	1.05	1.15	1.13	1.05	1.09
	1.06	1.04	1.05	1.13	1.05	1.09	1.06	1.00	1.04
90	1.15	1.10	1.13	1.22	1.09	1.17	1.15	1.06	1.10
	1.18	1.13	1.15	1.23	1.09	1.20	1.18	1.08	1.14
	1.11	1.07	1.08	1.17	1.09	1.13	1.10	1.03	1.07
95	1.18	1.13	1.16	1.25	1.11	1.22	1.18	1.08	1.15
	1.21	1.15	1.18	1.25	1.10	1.23	1.19	1.10	1.17
	1.13	1.19	1.11	1.24	1.12	1.17	1.13	1.05	1.09
100 [d]	1.30	1.20	1.30	1.35	1.16	1.35	1.26	1.16	1.26
	1.30	1.20	1.30	1.30	1.10	1.30	1.26	1.16	1.26
	1.20	1.16	1.20	1.35	1.16	1.35	1.20	1.10	1.20

[a] Based on discrete ordinates and Monte Carlo calculations; [b] based on discrete ordinates calculations; [c] based on Monte Carlo calculations.
[d] see footnote to Table 3.

when both methods are considered together, see Table 2), with spreads σ_u of about 10.5% and 9.9%. Again, the DO method tends to give a larger prediction uncertainty by about 7%. This is reflected in the safety factors given in Table 4 which are about 6% larger in the DO case than those based on the MC calculations. Based on JAERI's calculations, $\bar{u} \approx -1.1\%$ and $\bar{u} \approx -2.8\%$ (as opposed to approximately -2% when both methods are considered together) with spreads of about 6.5% and 7.8%. The DO method gives a larger calculated T_7 by about 2% than the value based on the MC method. Also notice from Table 4 that the US safety factors are larger than JAERI's by about 4%–15% at various confidence levels.

5.3. Line-integrated tritum production rate from natural lithium (T_n)

The prediction uncertainty in the line-integrated TPR from Li-n (T_n) was obtained in each experiment from uncertainties in the line-integrated TPR from Li-6 and Li-7 according to the procedures described by Eqs. (4)–(7). The NDF of the prediction uncertainty of T_n was constructed from these uncertainties and the mean uncertainty and its standard deviation were then calculated and introduced in Table 2. Distinction was also made between results based on the DO and MC calculations. The calculated prediction uncertainties based on these methods are shown in Table 3. Table 4 also shows the required safety factors for various confidence levels.

Based on the US calculations, the mean values $\bar{u}$ of T_n from the DO and MC methods are approximately 5.7% and 0.5% respectively (as opposed to about 3.3% when both methods are considered together, see Table 2), with spreads σ_u of about 7.6% and 7.0%. The DO method gives a larger prediction uncertainty by about 5%, as expected since these estimates are based on those obtained for T_6 and T_7 discussed above where this trend is observed. The safety factors are also larger by about 7%. Based on JAERI's calculations, $\bar{u} \approx -0.24\%$ and $\bar{u} \approx -4.0\%$ (as opposed to about -2.4% when both methods are considered together) with spreads of about 6.3% and 5.3%. The mean prediction uncertainty based on the DO method is larger by about 3% than the value based on the MC method and the safety

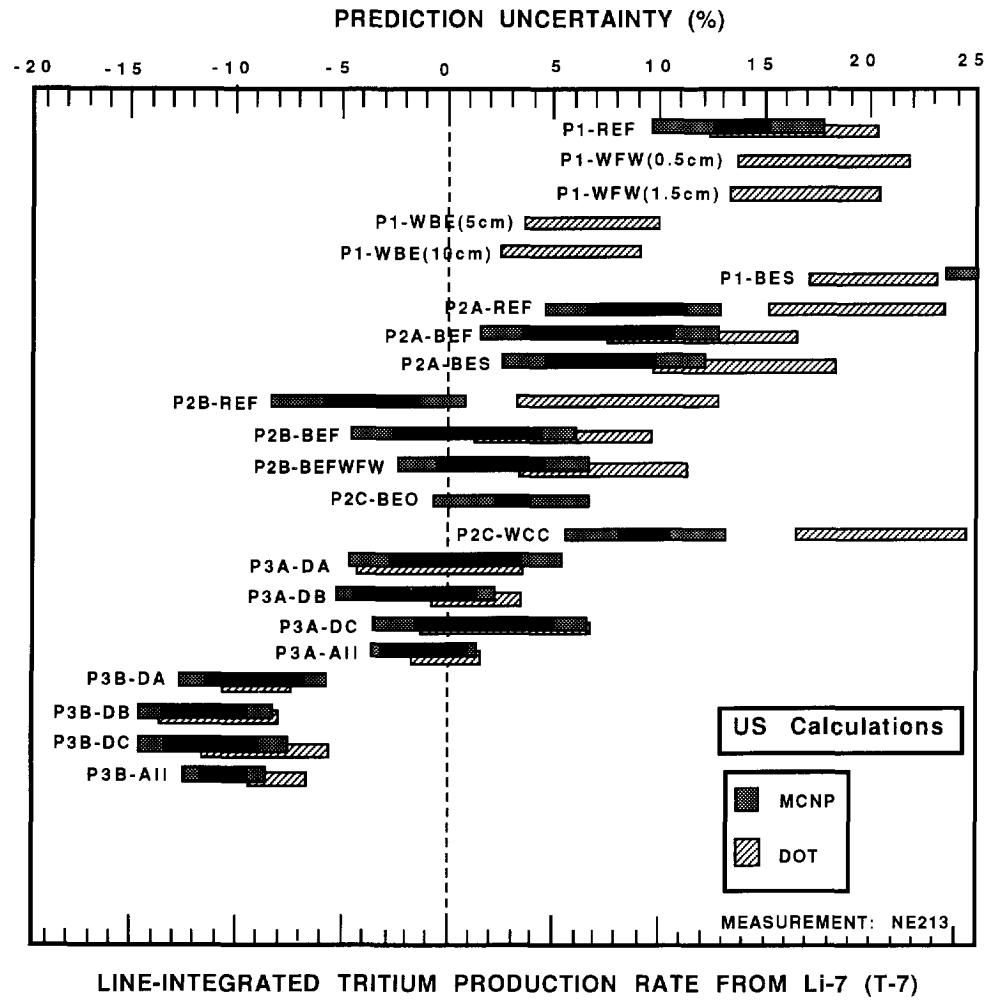

Fig. 12. The prediction uncertainty in tritium production rate from Li-7 (T_7) (US calculations, NE213 measurements).

factors are also larger by about 5%. The prediction uncertainty in T_n based on the US calculations is larger than that of JAERI's by approximately 6%, and the safety factors are also larger by about 8%.

6. Summary

Numerous fusion integral experiments were performed within the USDOE/JAERI Collaborative Program on Fusion Neutronics to quantify the uncertainty in prediction of the tritium production rate (TPR), as a prime design parameter in a fusion blanket. Various codes and nuclear data were used independently by the US and JAERI in analyzing these experiments. These experiments were conducted under various geometrical arrangements and different source conditions. They proceeded from a simple, one material test assembly to a more prototypical assembly that included the engineering features of a fusion blanket (e.g. first wall, coolant channels, multiplier...). A point neutron source as well as a simulated line source was used.

The calculational and experimental uncertainties (errors) in local TPR in each experiment i were propagated to estimate the prediction uncertainty u_i in the line-integrated TPR from Li-6 (T_6), Li-7 (T_7), and natural Li (T_n), along with the standard deviations σ_i. These results were based on measuring local T_6 by

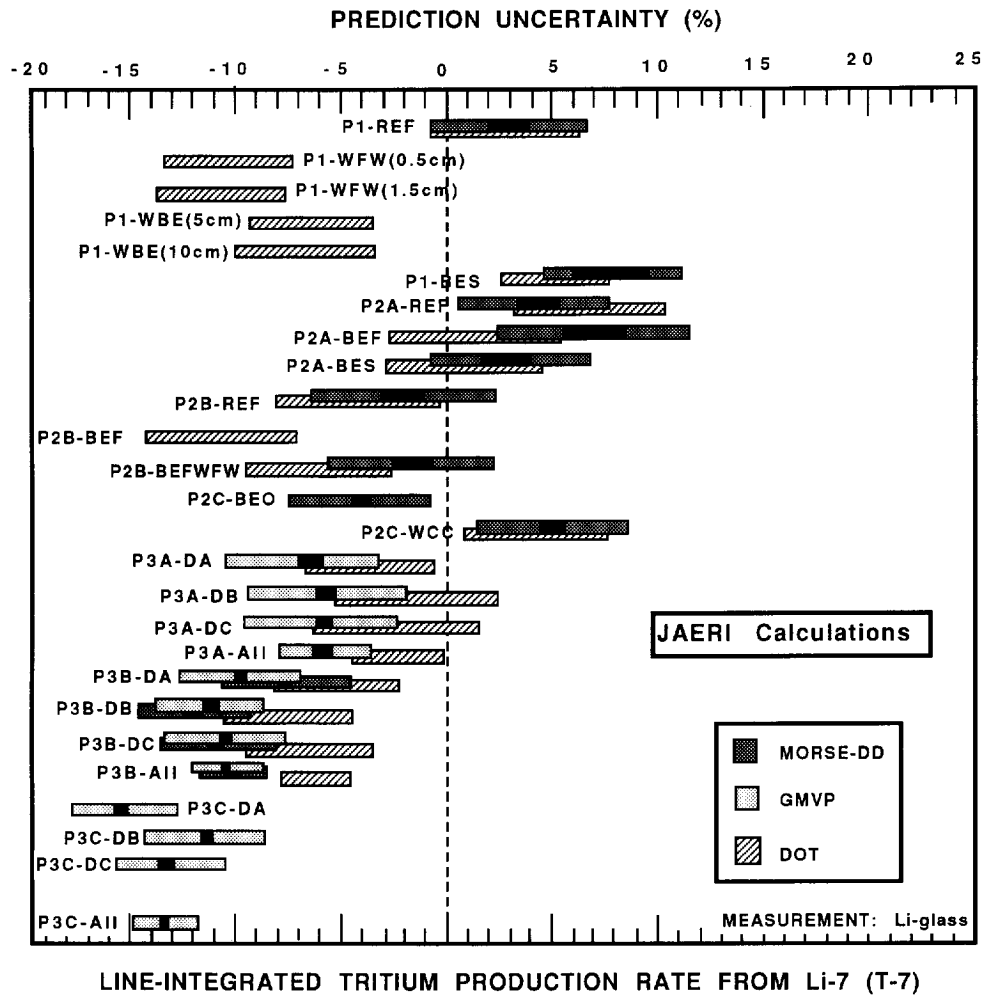

Fig. 13. The prediction uncertainty in tritium production rate from Li-7 (T_7) (JAERI's calculations, NE213 measurements).

Li-glass detectors and measuring T_7 by the NE213 method. The measured and calculated TPR from natural Li were obtained from T_6 and T_7. The methodology described in Ref. [3] was used to estimate quantitatively design margins and safety factors that fusion blanket designers can apply in TPR calculations based on the discrepancies observed between measurements and predicted values. Distinction was made between safety factors based on the US calculations, JAERI calculations, and both calculations considered simultaneously. Also, distinction was made between results based on the discrete ordinates (DO) and Monte Carlo calculations.

Based on considering all calculational and experimental methods used, the prediction uncertainty $\bar{u}$ in line-integrated T_6 is approximately 3.2% (US) and 0.2% (JAERI) with standard deviation $\pm\sigma_u$ of about 8%–9%. The uncertainties based on the US calculations are larger than JAERI's by about 2%–4%. If calculational methods are considered independently, it was shown in the US and JAERI calculations that the discrete ordinates (DO) method tends to give larger uncertainties (by about 6%–8%) than those based on the Monte Carlo method (MC). Not using safety factors, the probability that the calculated T_6 will exceed the actual value is about 62% (US) and about 54% (JAERI). To achieve the highest confidence level that calculated T_6 falls below actual value, the safety factors to be used were estimated to be approximately 1.3 (US) and 1.2

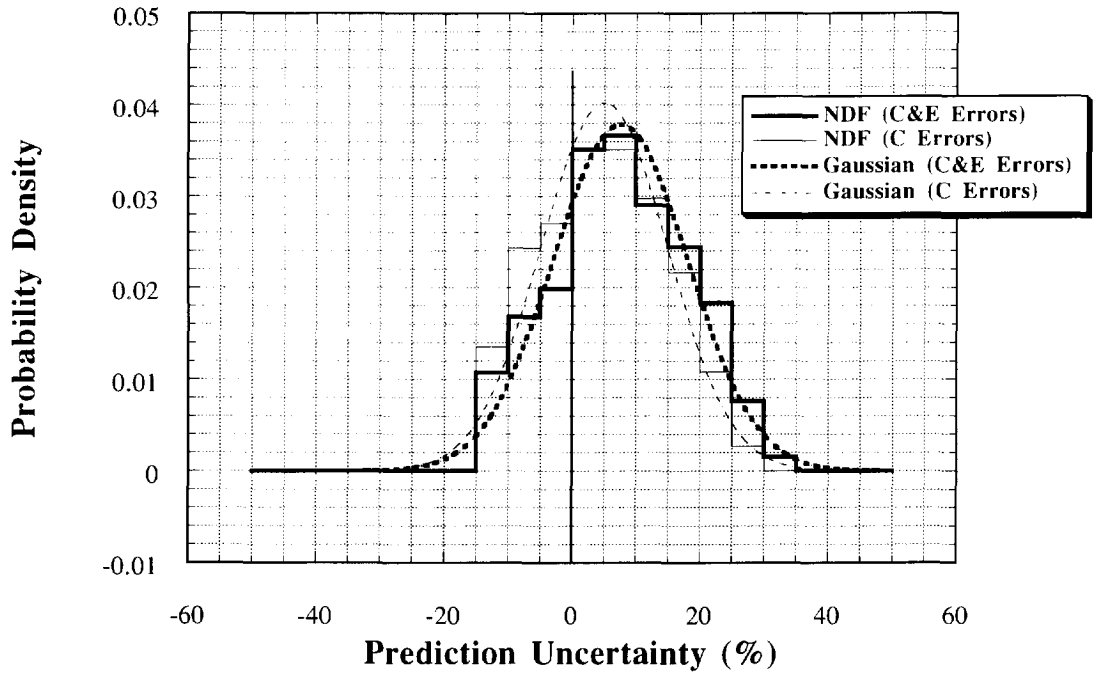

Fig. 14. Normalized density function f_j of the prediction uncertainty of T_7 (US codes and data, NE213 measurements, all phases).

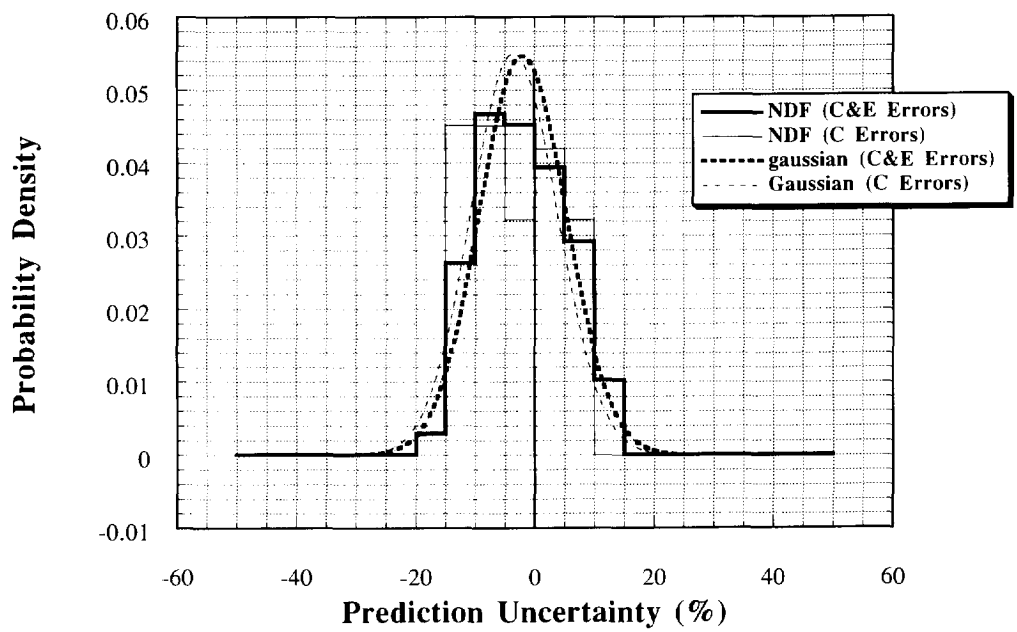

Fig. 15. Normalized density function f_j of the prediction uncertainty of T_7 (JAERI's codes and data, NE213 measurements, all phases).

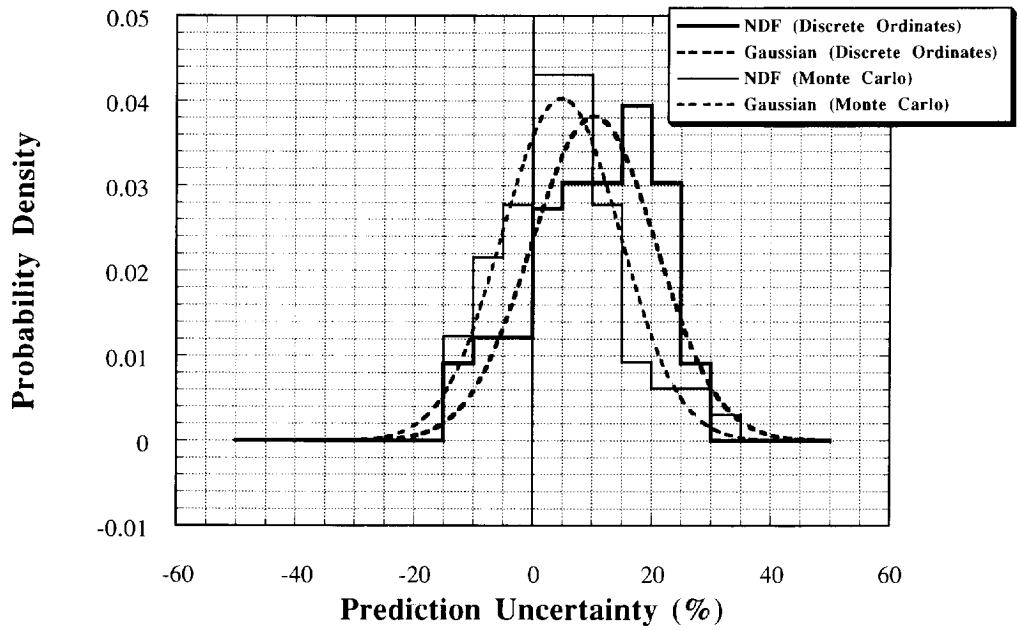

Fig. 16. The normalized density function of the prediction uncertainty in T_7 with distinction between calculational method (US calculations, NE213 measurements, all phases).

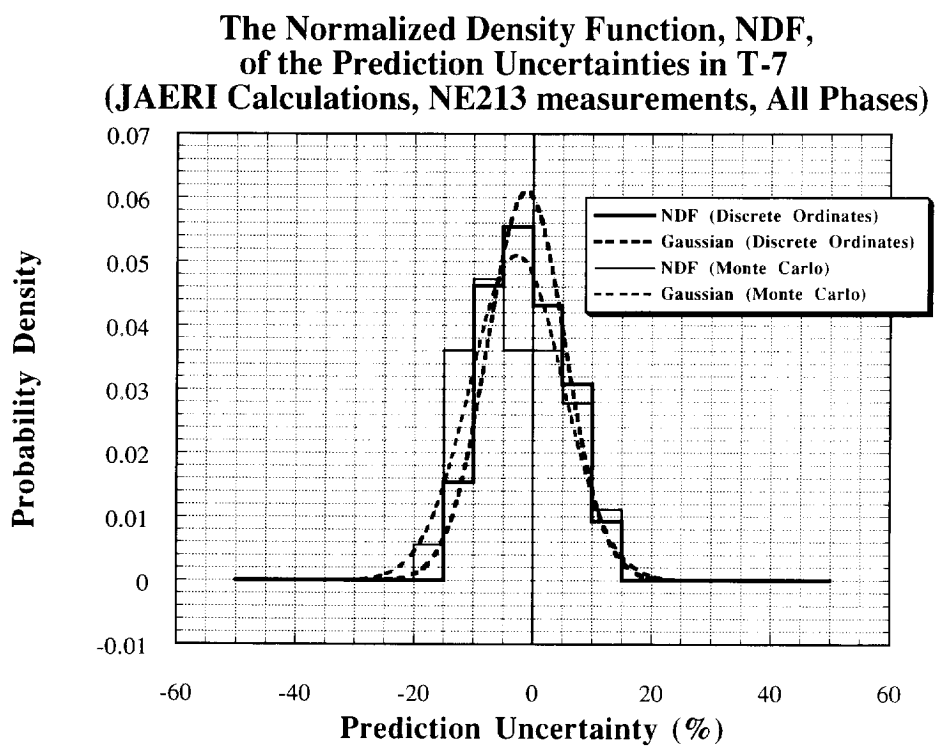

Fig. 17. The normalized density function of the prediction uncertainty of T_7 with distinction between calculational method (JAERI calculations, NE213 measurements, all phases).

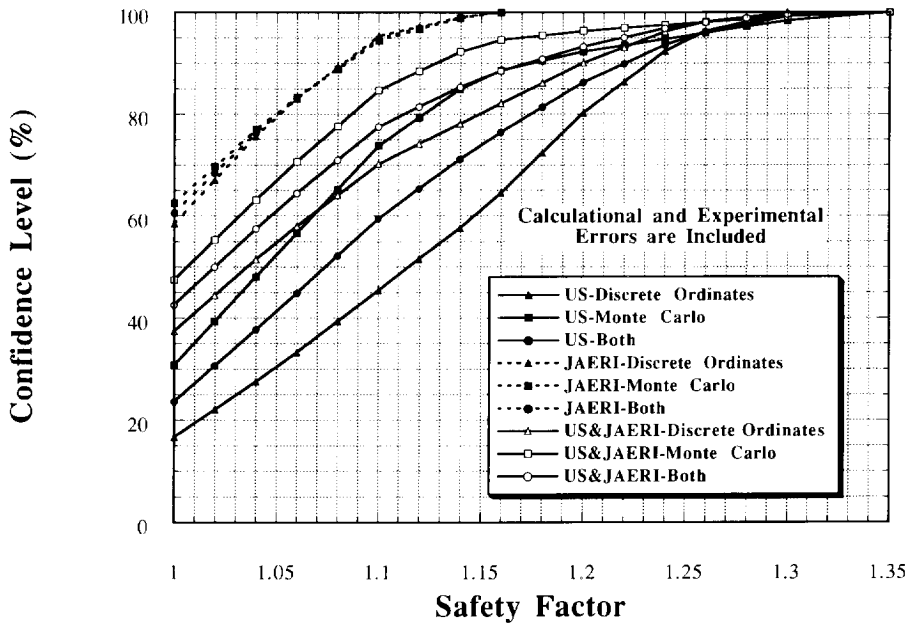

Fig. 18. Confidence level for calculations not to exceed measurements as a function of design safety factors for T_7 (NE213 measurements, all phases).

(JAERI). At lower confidence levels, the safety factors based on the US calculations are larger than those based on JAERI's calculations by about 4%–5%.

The mean prediction uncertainty $\bar{u}$ in the line-integrated T_7 is about 8% (US) and −2% (JAERI) with a spread $\pm\sigma_u$ of about 10% (US) and 7% (JAERI). The uncertainties based on the US calculations are larger than JAERI's by about 11%. The DO method gives larger uncertainties than the MC method by approximately 7% (US) and 2% (JAERI). If no safety factors are applied, the chance that the calculated T_7 will exceed the actual value is about 76% (US) and 40% (JAERI). To ensure that calculations are lower than actual values for T_7, the safety factor to be applied is approximately 1.35 (US) and 1.16 (JAERI). At lower confidence levels, the safety factors based on the US calculations are larger than those based on JAERI's calculations by about 4%–10%.

The mean prediction uncertainty $\bar{u}$ in the line-integrated TPR from natural lithium (T_n) is approximately 3.3% (US) and −2.4% (JAERI) with an estimated deviation around the mean value $\pm\sigma_u$ of about 8% (US) and 6% (JAERI). The uncertainties based on the US calculations are larger than those based on the MC methods by about 5% (US) and 3% (JAERI). Without applying a safety factor to T_n calculations, the probability that the calculated values are larger than measurements is about 62% (US) and 53% (JAERI). Applying a safety factor of approximately 1.26 (US) and 1.16 (JAERI) will ensure that calculations are below actual values.

Figs. 11 and 18 along with Table 4 can be used by blanket deisgners quantitatively to apply safety factors in the calculations of T_6, T_7, and T_n. These factors, however, are based on measured data obtained by Li-glass and NE213 detectors. Different factors are obtained when other measuring techniques are used [3,4]. For example, it was shown that the prediction uncertainties in T_6 will increase by about 2% when all techniques used to measure T_6 are considered [4]. This does not imply that the difference in T_6 measured by various techniques is about 2%, rather, the cases for which T_6 was measured by other techniques are fewer than the cases where measurements are performed by the Li-glass technique, and hence the prediction uncertainties in T_6 are dominated by results based on the Li-glass measurements. It was shown in Ref. [4] that differences of about 8% can be seen among various techniques used to measure T_6. It should be emphasized that the correction and safety factors cited here are applicable to TPR in Li_2O breeding material as obtained from the USDOE/JAERI Collabo-

rative Program and are based on simplified prototypical fusion blanket assemblies under various ideal neutron source conditions. An effort is needed to extrapolate these factors from integral experiments utilizing assemblies that replicate a particular fusion blanket/shield configuration to real fusion reactor conditions. This will require a dedicated research and development program focusing on achieving that goal.

References

[1] M.A. Abdou, E.L. Vold, C.Y. Gung, M.Z. Youssef and K. Shin, DT fuel self-sufficiency in fusion reactors, Fusion Technol., 9 (1986) 250–285.

[2] M.Z. Youssef and M.A. Abdou, Uncertainties in prediction of tritium breeding in candidate blankets designs due to present uncertainties in nuclear data base, Fusion Technol., 9 (1986) 286–307.

[3] M.Z. Youssef, A. Kumar, M.A. Abdou, Y. Oyama and H. Maekawa, Fusion integral experiments and analysis and the determination of design safety factors, part I: methodology, Fusion Technol., in press.

[4] M.Z. Youssef, A. Kumar, M.A. Abdou, Y. Oyama, C. Konno, F. Maekawa, Y. Ikeda, K. Kosako, M. Nakagawa, T. Mori and H. Maekawa, Fusion integral experiments and analysis and the determination of design safety factors, part II: application to the prediction uncertainty of tritium production rate from the USDOE/JAERI collaborative program on fusion blanket neutronics, Fusion Technol., in press.

[5] M.Z. Youssef, C. Gung, M. Nakagawa, T. Mori, K. Kosako and T. Nakamura, Analysis and intercomparison for phase I fusion integral experiments at the FNS facility, Fusion Technol., 10 (1986) 549–563.

[6] M.Z. Youssef, M.A. Abdou, C. Gung, R.J. Santoro, R.G. Alsmiller, J.M. Barnes, T.A. Gabriel, M. Nakagawa, T. Mori, K. Kosako, Y. Ikeda and T. Nakamura, Phase I fusion integral experiments, Vol. II, Analysis, UCLA-ENG-88-15, September 1988 (University of California, Los Angeles, CA); see also JAERI-M-88-177, August 1988 (Japan Atomic Energy Research Institute, Ibaraki).

[7] M.Z. Youssef, Y. Watanabe, C.Y. Gung, M. Nakagawa, T. Mori and K. Kosako, Analysis of neutronics parameters measured in phase II experiments of the JAERI/US collaborative program on fusion blanket neutronics, part II: tritium production and in-system spectrum, Fusion Eng. Des., 9 (1989) 323–332.

[8] M. Nakagawa, T. Mori, K. Kosako, T. Nakamura, M.Z. Youssef, Y. Watanabe, C.Y. Gung, R.T. Santoro, R.A. Alsmiller, J. Barnes and T.A. Gabriel, Analysis of neutronics parameters measured in phase II experiments of JAERI/US collaborative program on breeder neutronics, part I: source characteristics and reaction rate distribution, Fusion Eng. Des., 9 (1989) 315–322.

[9] Y. Oyama, S. Yamaguchi, K. Tsuda, Y. Ikeda, C. Konno, H. Maekawa, T. Nakamura, K.G. Porges, E.F. Bennet and R.F. Mattas, Phase IIB experiments of JAERI/USDOE collaborative program on fusion blanket neutronics, Fusion Technol., 15 (2, Part 2B) (1989) 1293–1298.

[10] M.Z. Youssef, Y. Watanabe, M.A. Abdou, M. Nakagawa, T. Mori, K. Kosako and T. Nakamura, Comparative analysis for phase IIA and IIB experiments of the US/JAERI collaborative program on fusion breeder neutronics, Fusion Technol., 15 (2, Part B) (1989) 1299–1308.

[11] M.Z. Youssef, M.A. Abdou, Y. Watanabe and P.M. Song, The US/JAERI collaborative program on fusion neutronics; phase IIA and IIB fusion integral experiments, The US analysis, UCLA-ENG-90-14, December 1989 (University of California, Los Angeles, CA).

[12] M. Nakagawa, T. Mori, K. Kosako, Y. Oyama and T. Nakamura, JAERI/US collaborative program on fusion blanket neutronics, analysis of phase IIA and IIB experiments, JAERI-M-89-154, October 1989 (Japan Atomic Energy Research Institute, Ibaraki).

[13] M.Z. Youssef, A. Kumar, M. Abdou, M. Nakagawa, K. Kosako, Y. Oyama and T. Nakamura, Analysis for heterogeneous blankets and comparison to measurements: phase IIC experiments of the USDOE/JAERI collaborative program on fusion neutronics, Fusion Technol., 19 (3) (1991) 1891–1899.

[14] Y. Oyama, S. Yamaguchi, K. Tsuda, C. Konno, Y. Ikeda, H. Maekawa, T. Nakamura, K. Porges and E. Bennet, Measured characteristics of Be multi-layered and coolant channel blankets: phase IIC experiments of the JAERI/USDOE collaborative program on fusion neutronics, Fusion Technol., 19 (3) (1991) 1955–1960.

[15] M.Z. Youssef et al., Phase-IIC experiments of the USDOE/JAERI collaborative program on fusion blanket neutronics—experiments and analysis of the heterogeneous fusion blankets, Vol. II, Analysis, UCLA-FNT-64, UCLA-ENG-93-19, December 1992 (University of California at Los Angeles, CA); see also M. Nakagawa et al., JAERI-M-92-183, December 1992 (Japan Atomic Energy Research Institute, Ibaraki).

[16] M.Z. Youssef et al., Nuclear analysis of integral experiments on Li_2O test assembly with local heterogeneities utilizing 14 MeV neutron source, Fusion Technol., in press.

[17] Y. Oyama et al., Neutronics integral experiments on lithium-oxide fusion blanket with heterogeneous configurations using D–T neutrons, Fusion Technol., in press.

[18] T. Nakamura, Y. Oyama, Y. Ikeda, C. Konno, H. Maekawa, K. Kosako, M. Youssef and M. Abdou, A line D–T neutron source facility for annular blanket experiment: phase III of the JAERI/USDOE collaborative program on fusion neutronics, Fusion Technol., 19 (3) (1991) 1873–1878.

[19] Y. Oyama, C. Konno, Y. Ikeda, H. Maekawa, K. Kosako, T. Nakamura, A. Kumar, M. Youssef, M. Abdou and E. Bennet, Annular blanket experiment using a

line DT neutron source: phase IIIA of the JAERI/US-DOE collaborative program on fusion neutronics, Fusion Technol., 19 (1991) 1879–1884.

[20] M.Z. Youssef, Y. Watanabe, A. Kumar, Y. Oyama and K. Kosako, Analysis for the simulation of a line source by a 14 MeV moving point source and impact on blanket characteristics: the USDOE/JAERI collaborative program on fusion neutronics, Fusion Technol., 19 (1991) 1843–1852.

[21] Y. Oyama, C. Konno, Y. Ikeda, H. Maekawa, K. Kosako, T. Nakamura, A. Kumar, M.Z. Youssef and M.A. Abdou, Phase III experimental results of JAERI/USDOE collaborative program on fusion neutronics, Fusion Eng. Des., 18 (1991) 203–208.

[22] M.Z. Youssef, A. Kumar, M.A. Abdou, Y. Oyama, K. Kosako and T. Nakamura, Post-analysis for the line source phase IIIA experiments of the USDOE/JAERI collaborative program on fusion neutronics, Fusion Eng. Des., 18 (1991) 265–274.

[23] M.Z. Youssef, M.A. Abdou, A. Kumar, L. Zhang, K. Kosako, Y. Oyama, F. Maekawa, Y. Ikeda, C. Konno and H. Maekawa, The nuclear performance of an annular Li_2O blanket system surrounding an artificially simulated 14 MeV line source and comparison of calculations to measurements, Fusion Technol., in press.

[24] Los Alamos Monte Carlo Group, MCNP—a general Monte Carlo code for neutron and photon transport, version 3A, LA-7396, Rev. 2, 1986 (Los Alamos National Laboratory, Los Alamos, NM).

[25] W.A. Rhoades and R.L. Childs, An updated version of the DOT 4 (version 4.3) one- and two-dimensional neutron/photon transport code, ORNL-5851, April 1982 (Oak Ridge National Laboratory, Oak Ridge, TN); see also CCC-429, 1982 (Radiation Shielding Information Center, RSIC).

[26] L.P. Ku and J. Kolibal, RUFF—a ray tracing program to generate uncollided flux and first collision source moments for DOT4, A User's Manual, EAD-R-16, 1980 (Plasma Physics Laboratory, Princeton University, Princeton, NJ).

[27] R.A. MacFarlane, TRANSX-CTR: a code for interfacing MATXS cross-section, libraries to nuclear transport codes for fusion systems analysis, LA-9863-MS, February 1984 (Los Alamos National Laboratory, Los Alamos, NM).

[28] P.G. Young et al., Evaluated data for n + 9Be reactions, LA-7932-MS, July 1979 (Los Alamos National Laboratory, Los Alamos, NM).

[29] M. Nakagawa and T. Mori, MORSE-DD, a Monte Carlo code using multigroup double differential form cross-sections, JAERI-M84-126, July 1984 (Japan Atomic Energy Research Institute, Ibaraki).

[30] T. Mori, M. Nakagawa and M. Sasaki, Vectorization of continuous energy Monte Carlo method for neutron transport calculation, J. Nucl. Sci. Technol., 29 (4) (1992) 325–336.

[31] Y. Ikeda and M.Z. Youssef, Two dimensional cross-section sensitivity and uncertainty analysis for tritium production rate in fusion-oriented integral experiments, Fusion Technol., 13 (1988) 616–643.

[32] P.M. Song, M.Z. Youssef and M.A. Abdou, New approach and computational algorithm for sensitivity/uncertainty analysis for SED and SAD with application to beryllium integral experiments, Nucl. Sci. Eng., 113 (1993) 339–366.

[33] M.Z. Youssef and Y. Oyama, Required design margins and their economic impact in fusion reactors to compensate for nuclear data uncertainties—a global approach to define safety factors based on integral experiments, Proc. Int. Conf. on Nuclear Data for Science and Technology, 9–13 May 1994, Gatlinburg, TN.

[34] Y. Oyama, K. Kosako, C. Konno, Y. Ikeda, F. Maekawa and H. Maekawa, Influence of selection of calculation parameters in discrete ordinate code DOT3.5 for analysis of fusion blanket integral experiments in JAERI/USDOE collaborative program, Fusion Eng. Des., 28 (1995).